Experimental Thermal and Fluid Science 126 (2021) 110399

Contents lists available at ScienceDirect

Experimental Thermal and Fluid Science

journal homepage: www.elsevier.com/locate/etfs

High-resolution concentration measurement in water/n-butanol binary system by means of high-frequency electrical impedance method

Wassilis Tzevelecos [a], Quentin Galand [a], Sotiris Evgenidis [b], Konstantinos Zacharias [b], Thodoris Karapantsios [b,*], Stefan Van Vaerenbergh [a]

[a] Université libre de Bruxelles (ULB) - Service de Chimie Physique, B1050 Brussels, Belgium
[b] Department of Chemical Technology and Industrial Chemistry, Faculty of Chemistry, Aristotle University, University Box 116, 541 24 Thessaloniki, Greece

ARTICLE INFO

Keywords:
I-VED
Concentration diagnostic
Binary mixture
SELENE
High-frequency impedance method

ABSTRACT

Chemical composition measurement technologies for binary systems are needed in many industrial and research applications for monitoring fluid composition in pipes and sample analysis. Except for spectroscopy technology, composition measurement is retrieved by monitoring fluid properties as refractive index, density, electrical conductivity or fluid sound velocity. Demanding applications are those where optical access to the fluid is not easy or available, very local or/and fast measurements are required, and where space limitations dictate the use of sub-millimeter non-intrusive sensors. Combination of all the above constraints in one application makes it extremely difficult to cope with. The latter is the motivation for the present work where a novel diagnostic method, based on I-VED (In-Vivo Embolic Detector) patented technology used in humans for the diagnosis of Coronary Artery Disease and Decompression Sickness, is implemented to determine the concentration of a binary mixture using high frequency impedance measurements. At first, the technology allows tuning over a range of excitation frequencies to identify a proper signal where the fluid attains chiefly an ohmic behavior. Then it retrieves chemical composition of the binary system through calibration curves with respect to resistance and temperature. Adaptation of the I-VED as concentration sensor has been driven by the necessity to integrate such a diagnostic in setups where available solutions in literature cannot be applied. Further to satisfying the aforementioned constraints, I-VED offers also other advantages compared to existing technologies as it provides high-scale resolution, it is not sensitive to electromagnetic interference (EMI) and it retrieves an integrated signal of the liquid between the electrodes, so localization of the measuring volume can be controlled. The proposed method has been tested in aqueous solutions of alcohol and its dependence on temperature and alcohol concentration has been investigated at an existing experimental setup named SELENE (SELf-rewetting fluid for ENErgy management), developed for heat transfer research applications.

1. Introduction

Concentration diagnostics for binary systems used in laboratories and industrial applications can be essentially grouped in six different families: sonic velocity method, density method, conductivity method, refractometry method (as interferometry), radiometry and spectroscopy method [1]. Most of the listed methods consist of monitoring fluid properties to retrieve, after previous calibration or with respect to reference fluid configuration, the needed chemical composition. In addition, since the considered monitored liquid properties are temperature dependent, thermal sensors must be coupled with concentration probes.

When handling setups where the concentration variation along the system must be measured and composition analysis by sampling is not possible, it is convenient to have an easy-to-integrate concentration diagnostic, providing fast and robust measurements. For this type of applications, refractometry method as the one developed by PROMETE and reported in [2] or FISO [3] may be a solution; however the scale resolution of such techniques is limited and may not fit experimental requirements. In addition, these techniques provide solely local concentration measurements since the sensitive area is the interface between the probe and the liquid.

In order to overcome all these limitations, a different type of impedance method based on I-VED (In-Vivo Embolic Detector)

* Corresponding author.
E-mail address: karapant@chem.auth.gr (T. Karapantsios).

https://doi.org/10.1016/j.expthermflusci.2021.110399
Received 15 December 2020; Received in revised form 3 March 2021; Accepted 14 March 2021
Available online 19 March 2021

hardware is investigated herein. I-VED is a technology patented by the Aristotle University of Thessaloniki (AUTh) [4] based on ultra-sensitive AC (Alternating Current) impedance spectroscopy. I-VED has been originally developed for medical applications (initially bubbles detection during Decompression Sickness, e.g., in astronauts and scuba divers, and also assessment of endothelial functionality for the diagnosis of Coronary Artery Disease [5]) but its use has been extended to several engineering two-phase (gas-liquid) applications for gas fraction and average bubble size estimation [6–11].

Here, I-VED is adapted to determine the concentration of different components in liquid-liquid systems. The electrical impedance of a liquid mixture varies with component concentrations, temperature, excitation frequency and liquid measuring volume crossed by the AC excitation current. All these factors and the way they vary with respect to operational conditions must be taken into account in order to retrieve meaningful information. The most critical aspect in impedance measurements for composition measurement is to differentiate among the conductive, capacitive, and inductive components of the signal: a) to avoid electrodes polarization and b) because these components vary differently with respect to concentration of substances. The most common way is to sort out the conductive component by identifying a proper excitation frequency that suppresses the capacitive and inductive components of the impedance signal. In cases of mixtures where water is one component, it helps to add a minimal amount of electrolyte to increase the conductivity contrast of water with the other component(s). Starting with a considerably conductive baseline solution (i.e. an aqueous solution of electrolyte), the addition of a third component, e.g. an alcohol, usually reduces the solution conductivity because of solution dilution and chemical effect of the alcohol molecule. Retrieving the relationship between the solution conductivity and alcohol concentration allows determining the concentration of such component in the system. Such a concentration diagnostic method permits fast composition measurement localized in just the liquid volume between the excitation electrodes.

I-VED adaptation for concentration measurements has been investigated in aqueous solutions of alcohol at different configurations in SELENE setup to determine signal dependence with temperature and alcohol concentration. SELENE (SELf-rewetting fluid for ENErgy management) is an experimental setup built to test fluids for thermal management in space applications [12]. Apart from the technical and functional validation of the proposed I-VED adaptation, a comparison is performed with existing technologies to demonstrate the achieved scale resolution with respect to the FISO probe accuracy and the PROMETE sensor from the data reported by [2].

2. Materials and methods

2.1. I-VED breadboard setup

I-VED tests are performed after integrating the measuring system into the SELENE experimental hardware. The latter consists of a Brass 190 mm long groove with trapezoidal cross-section. Heat is transferred along the groove by two-fold phase change: (i) evaporation of the test fluid at the hot end of the groove and flow of the generated vapor to the cold end driven by the volume expansion upon phase change, (ii) condensation at the cold end of the groove and flow of the condensate back to the hot end driven by capillary forces [13]. The SELENE phase change loop and the cross-section dimensions are shown in Fig. 1. When performing tests under isothermal conditions to determine I-VED sensitivity, the groove is inserted into a simplified plastic structure. Two pairs of I-VED electrodes are located into the sidewalls of the groove cross sections as shown in Figs. 2 and 3; this configuration allows obtaining an average value of the concentration for the liquid contained between the electrodes. Each electrode consists of a metal wire of 0.9 mm diameter inserted into a Teflon® tube with external diameter of 1.5 mm; for the preliminary experiments reported here, when a SELENE brass channel is considered the electrode wires are made of Copper.

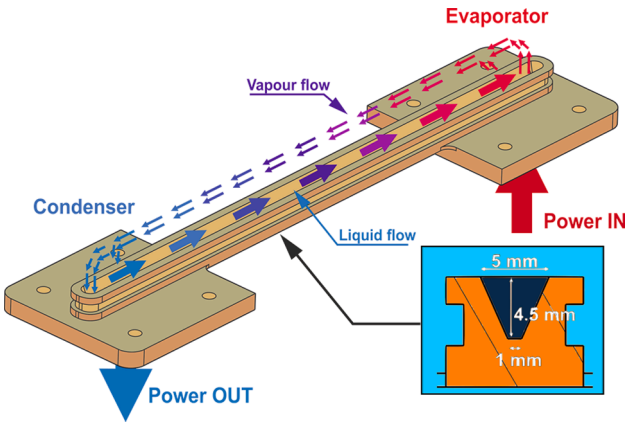

Fig. 1. SELENE phase change loop and section dimensions.

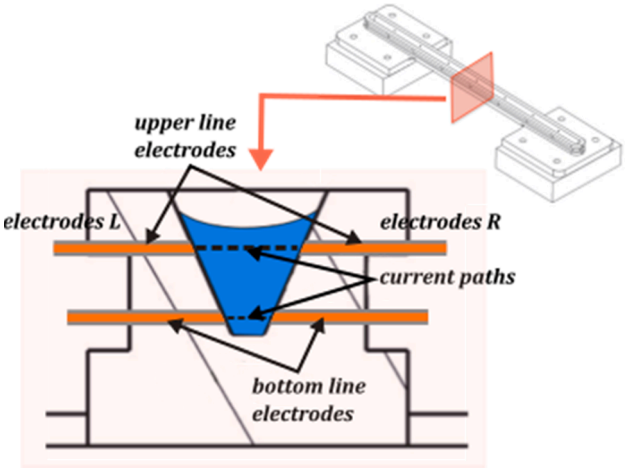

Fig. 2. Sketch of the electrodes position inside SELENE channel cross-section: there are two pairs of electrodes (upper and bottom electrodes, henceforth referred to as UP and DOWN). Each electrode consists of a metallic core surrounded by a Teflon® layer to avoid electrical contact between the core and the metallic groove.

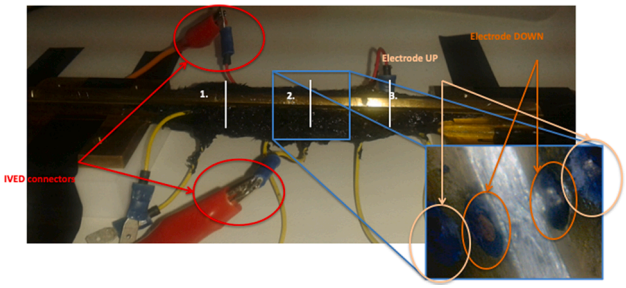

Fig. 3. Setup used to measure I-VED sensitivity in isothermal conditions: in red are marked the I-VED connectors to the left and right electrodes, in white are numbered the position of the electrode stations along the groove and in light and dark orange the electrodes inside the groove from a magnified photo of the inside of the groove taken from the top. (For interpretation of the references to colour in this figure legend, the reader is referred to the web version of this article.)

When the experiment is performed at elevated temperatures, it is necessary to modify the experimental SELENE hardware in order to minimize vapor loss of the liquid evaporating in the channel and to collect the correct I-VED signal evolution. In this case, Figs. 4 and 5, the

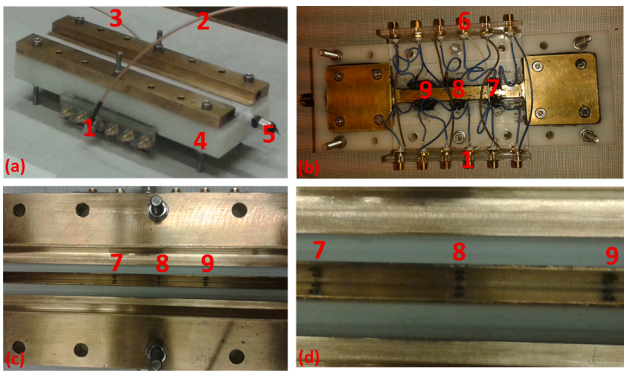

Fig. 4. (a) SELENE breadboard with I-VED electrodes integrated (Nr. 2 and 3 refer to right and left cables) without GLASS and COVER parts; Nr. 1 is the electrode SMA (SubMiniature version A) connector while Nr. 4 and 5 are the CASE part and the liquid filling fitting, (b) Bottom view of the breadboard with left and right SMA connectors (Nr. 1 and 6) and position of the three stations where electrodes are inserted (Nr. 7, 8 and 9), (c) Top view of the electrodes inside the channel, two pairs of electrodes per section, (d) Details of the electrodes of the stations Nr. 7, 8 and 9.

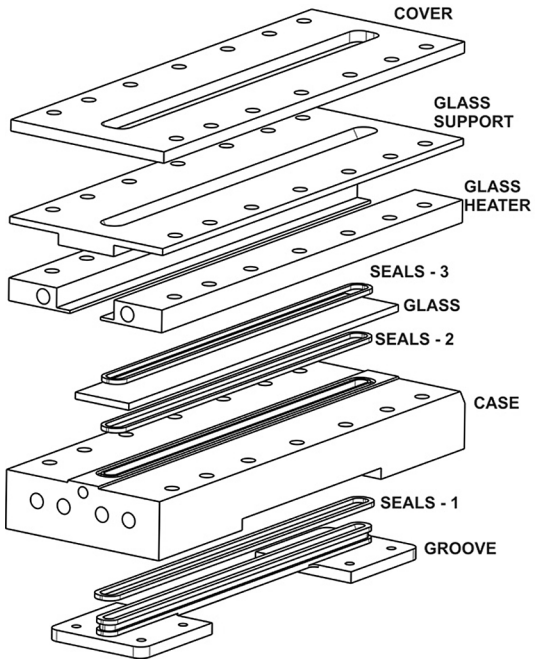

Fig. 5. Exploded CAD view of the setup used for I-VED tests performed with thermoregulation of the setup.

brass channel is integrated in the PA-66 plastic part (named CASE in Fig. 5) as an equivalent to the PEEK part of SELENE experimental hardware [13]. Between the groove and the CASE, a rubber seal made of Viton (SEAL-1) is placed to avoid liquid leakage. Above the CASE, GLASS and GLASS HEATER are properly mounted; the thermal contact between GLASS HEATER and GLASS is ensured by adding thermo-conductive paste. SEAL–2 and SEAL–3 are used to reduce the vapor loss when performing experiments at high temperatures. The GLASS SUPPORT and the COVER are utilized to squeeze the GLASS seals. The condensation on the internal side of the GLASS window is prevented by the GLASS HEATER part that is warmed with water recirculation. PA-66 plastic CASE is also heated by warm water recirculation to prevent vapor condensation on the internal walls of the vapor area inside the SELENE breadboard. In addition, to prevent oxidation of the electrodes that may be faster at elevated temperature, the electrode Copper core wires have been replaced with Platinum ones of the same diameter.

2.2. I-VED hardware setup

The hardware used for I-VED laboratory experiments (Figs. 2 and 3) consists of an AC signal generator (SG) used as a sinusoidal voltage source excitation, a data acquisition card AudioBox (AB), a decade resistance box (RB) for signal tuning and a computer connected to the AudioBox to monitor in real time and record output signals (Figs. 6 and 7). The principle of I-VED technology is based on the comparison between the input voltage from the SG and the output voltage drop caused by the AC current passing through the liquid between two electrodes integrated in the groove test cell. The output is a data file that can be converted into a resistance time series of high sampling frequency and resolution by the corresponding algorithm. I-VED algorithm is also used to reject the EMI noise thanks to narrow-band filtering of the input and output signals. Although I-VED can provide resistance time series of several thousands data per second at a resolution better than 0.01%, for the needs of the present application and the time scale of the experiment, it has been decided to set the sampling frequency to 200 Hz. The output resistance resulting from the processing algorithm is directly associated with the mixture's electrical conductivity k and, consequently, to alcohol concentration and temperature by proper calibration.

A Teflon® tube surrounding the metallic wire core of each electrode is ensuring electrical insulation between electrode core and channel and must be thick enough to avoid any stray currents induced by the SG.

The representative electrical equivalent circuit for a pair of electrodes of Fig. 2 can be seen in the drawing of Fig. 8, where the resistances of SELENE breadboard R_c and decay box (RB) R_t are connected in series. The equivalent input impedance Z_{AB} (0.5 MΩ) of the AudioBox (AB) can be modeled as the parallel connection of the resistance R_a and capacitance C_a.

In the circuit shown in Fig. 8, the inputs of the AudioBox are connected to the decay box (RB) and to the signal generator (SG); the voltages after and before the SELENE breadboard (V_L and V_R refers to "left" and "right" port of the data acquisition device) are so the inputs of the AudioBox that gives the measured signal S_{dB} in dB as:

$$S_{dB} = 20log_{10}V_i \tag{1}$$

with V_i being the voltage ratio between V_L and V_R that can be expressed as:

$$V_i = \frac{R_t}{R_c + R_t} \tag{2}$$

where R_t is the "terminal" resistance of the decay box that can be tuned manually and R_c is the resistance of the channel that depends on the liquid composition between I-VED electrodes. Tuning the terminal resistance R_t, the output signal S_{dB} is regulated to lie in the range of higher sensitivity for I-VED processing algorithm that corresponds to the range where the electrical response of the AudioBox is almost linear. This region is checked experimentally by analyzing the response of the system when increasing the conductivity of the solution between the

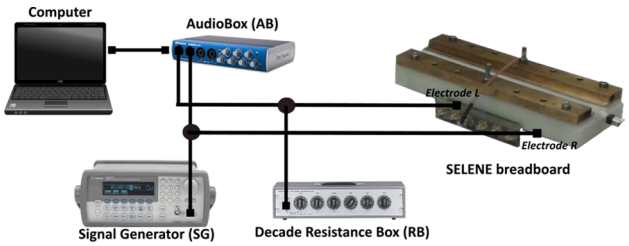

Fig. 6. Scheme of the I-VED setup for concentration measurement.

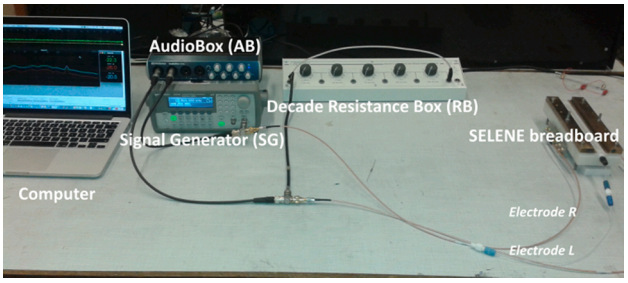

Fig. 7. Photo of the laboratory setup for I-VED.

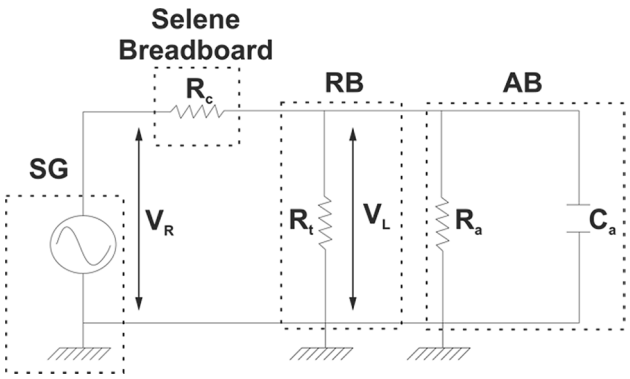

Fig. 8. Electrical equivalent circuit of the experimental setup.

electrodes.

In order to reject any electromagnetic interference or extraneous noise from the measured signals, the frequency of the sinusoidal signal generator is set at 25 kHz (after a frequency scanning from 10 to 100 kHz) and the amplitude at 2 V_{rms} (root mean square value). The selected frequency and amplitude optimize the signal/noise ratio: 25 kHz are too far from the mains interference region of 50 Hz (low frequency noise) and 2 V_{rms} are much higher than the inherent measurement noise.

2.3. I-VED signal dependence analysis

Considering the case of theoretical ideal conditions, i.e. the electric field is uniform and there is no diffusion field between the electrodes, the electrical current lines are flowing from one electrode to another at the opposite side of the groove following the path described by an imaginary cylinder connecting the two facing electrodes. As a result, the voltage between the electrodes is given by Ohm's law:

$$V = R_{ci} I \tag{3}$$

where R_{ci} is the ideal resistance between the electrodes and I is electrical current flowing through R_{ci}. Boundary conditions dictate that the electric field **E** is normal at the conductive surface of the electrodes and, according to Faraday's law, any line integral of electric field **E** from one electrode to another equals the voltage V regardless the path of integration. Considering a conductive medium with uniform conductivity σ anywhere between the electrodes and a uniform electric field parallel to the axis of the electrodes (Fig. 2), the voltage is:

$$V = \int_0^l \boldsymbol{E} d\boldsymbol{l} = El \tag{4}$$

where l is the distance between the electrodes. The electric field **E** induces a current density **J** in the conductive medium which is:

$$\boldsymbol{J} = \sigma \mathbf{E} \tag{5}$$

The integral of current density **J** over the electrode surface A is the total current I, thus:

$$\mathrm{I} = \iint_A \boldsymbol{J} d\boldsymbol{A} = \iint_A \sigma \mathbf{E} d\boldsymbol{A} = \sigma \mathrm{EA} \tag{6}$$

Substituting the equations (4) and (6) into equation (3), it is obtained:

$$R_{ci} = \frac{1}{\sigma}\frac{l}{A} = \rho \frac{l}{A} \tag{7}$$

where ρ is the resistivity of the mixture, l is the distance between the two electrodes and A is the cross-sectional area of the imaginary cylinder connecting the two electrodes. Although the electric field was considered uniform and confined between the electrodes, it diverges and reaches a diffusion field in real applications such as the SELENE channel. Hence, the actual ratio l/A is different from that defined based on the geometrical dimensions. In order to take into account any deviation from the ideal conditions, the equation (7) needs to be modified with the introduction of a correction coefficient. Therefore the actual total resistance R_c linked to the portion of liquid lying between the two electrodes and is equal to:

$$R_c = \rho \frac{l}{A} c_f \tag{8}$$

where ρ is the resistivity of the mixture, l is the distance between the two electrodes, A is the cross-sectional area of the imaginary cylinder connecting the two electrodes and c_f a correction coefficient defined below. The ratio l/A is named cell factor and it is also denoted as K. $l \times A$ corresponds to the imaginary cylinder liquid volume within which electrical currents flow. Yet, this assumption is not respected in case of reducing overall mixture conductance (e.g., by reducing dissolved electrolyte or by increasing second component concentration at given temperature). In this last case, the above equation needs a correction taking into account the deformation of the cylindrical volume between the electrode pair and the stray currents between each electrode and the metallic channel casing. This is also the case when the liquid meniscus (sketched in Fig. 2) interferes with that volume. However, due to the complexity in modelling the electrical currents for a non-nominal case, it is preferred instead to increase the conductivity of the baseline aqueous solution of electrolyte to minimize the abovementioned effects. All in all, c_f in equation (8) can be considered as a compensation term that depends on: a) the chemical composition of test liquid and b) the interaction of test liquid with the applied frequency of AC excitation. Sometimes, for convenience, c_f is included in the geometrical terms of the equation (8). However, in the case of measurements for low concentrations of electrolyte solutions at high frequency, c_f may change considerably as observed by Bulavin et al. [14] at given temperature conditions for aqueous solutions of NaCl of varying concentration (1.8, 4.5 and 9 g/l), Fig. 9. In this plot, the curves converge to an asymptotic value as the frequency increases and the convergence is faster for low concentration solutions. This means that for liquids with conductivity in the range of 100–200 μS/cm (~0.05–0.10 g NaCl per liter of aqueous solution, see Fig. 10), an excitation frequency of 25 kHz, like in the present configuration of I-VED, assures that the conductivity of the liquid does not exhibit any frequency dependence. For this reason, c_f can be considered equal to 1.

The measured resistance, R_c, includes the resistance of the solution and the contact impedance Z_C between the electrodes and the solution. Z_C can be modelled as a capacitive component C_{DL} connected in parallel with the series connection of resistive components R_{CT} and Z_W, i.e. $Z_C = X_{CDL}//(R_{CT} + Z_W)$ [15], where C_{DL} is the double layer capacitance with reactance X_{CDL}, R_{CT} is the charge transfer resistance and Z_W is Warburg impedance. The polarisation resistance can be neglected when employing an AC excitation signal of 25 kHz. At high excitation frequencies, the reactance X_{CDL} becomes very low, essentially short

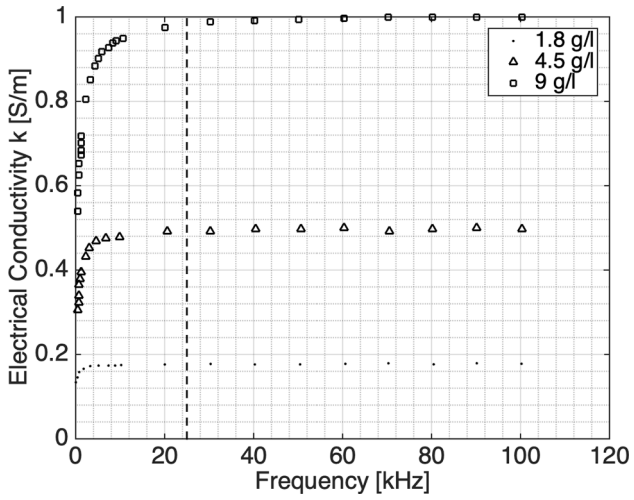

Fig. 9. Electrical conductivity k dependence on excitation frequency for aqueous solutions of NaCl of varying concentration [14]. The selected excitation frequency of 25 kHz is denoted by a vertical dashed line.

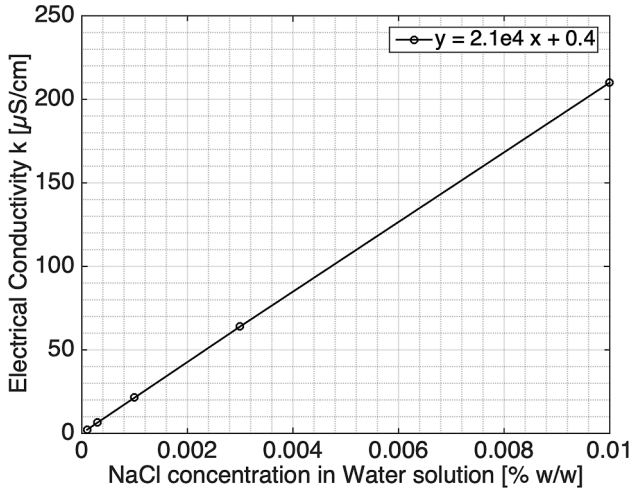

Fig. 10. Electrical conductivity of aqueous solution of NaCl as a function of salt concentration [17] at 25 °C.

circuiting the combination $R_{CT} + Z_W$ and, eventually, the cell impedance equals to the solution resistance [16]. The typical values of double layer capacitance are in the range 10 – 40 μF/cm^2 and depend on the ion concentration as well as the material of the electrodes. Considering the surface area of the electrode, the excitation frequency of 25 kHz and an average C_{DL} = 25 μF/cm^2, the reactance X_{CDL} equals to 40 Ω. The electrode impedance would be even lower due to the parallel connection of X_{CDL} with the resistive components. Therefore, Z_C is several orders of magnitude lower even from the lowest resistance of the solution. In order to further minimize the effect of contact impedance and obtain the maximum measurement accuracy, the measured resistance of the solution is calibrated against known concentrations of n-butanol, so any effect of this miniscule Z_C is taken into account.

Addition of salt is fundamental in order to discretize the information coming from the breadboard in Fig. 8 with respect to the SG and AB internal resistances. The range of high sensitivity for I-VED should correspond to the output signal region (in dB), where the Z_{AB} impedance, given by both R_a and C_a, shows a linear dependence with R_c and R_t variations, i.e. when $Z_{AB} \gg R_t$.

The baseline solutions has been prepared, accordingly, by mixing 4.7×10^{-3}% and 9.5×10^{-3}% w/w of NaCl in water. The dependence of the mixture conductivity k with salt concentration at 25 °C is almost linear as shown by Fig. 10 interpolating data from [17]. Such small quantity of salt does not influence the surface tension of water.

The liquid resistivity ρ (or equivalently the liquid electrical conductivity k) is a function of temperature and concentration while the other terms in equation (8) are fixed when working at nominal conditions and at a fixed excitation frequency. In fact, the cell factor is a geometrical quantity and varies differently for each pair of electrodes. So it is determined experimentally only once.

Since the conductivity-meter (HANNA) used to monitor the electrical conductivity of solutions works at 1 kHz while I-VED performs measurements at 25 KHz, it is in principal necessary to assess the error committed depending on c_f. Table 1 reports the resistance values obtained with I-VED setup and with an inductance (L), capacitance (C), resistance (R) measurement LCR bridge (LCRB) operating at 1 kHz, for the bottom line electrodes shown in Fig. 2 at various solution compositions and at ambient temperature considering Brass SELENE channel with Copper electrodes. As shown, when increasing the solution conductivity, the difference of the two values increases as well; each solution corresponds to a different curve in Fig. 9 from which the readings for I-VED at 25 kHz and for LCRB at 1 kHz are taken. The deviation between readings at the two frequencies are not much apart but still it has to be taken into account. Adding a second component of different conductivity, e.g. alcohol, to the baseline solution affects the solution conductivity. So the different values of resistance in Table 1 may be viewed also as the effect of a second component at different concentrations.

For a given aqueous solution of NaCl, as mentioned above, the conductivity is only a function of temperature and second component concentration. Therefore, in order to determine alcohol concentration from I-VED resistance measurements, a calibration is needed to correlate alcohol concentration and temperature with the conductivity of the considered solution. Calibration corresponds in retrieving the surface plotted in Fig. 11, obtained by fitting experimental data collected at different second component concentrations and temperatures using commercial HANNA conductivity meter at 1 kHz. As second component, n-butanol has been chosen that yields a Self-Rewetting Fluid (SRF) [18] when mixed with water; this specific liquid mixture is investigated as working fluid in the SELENE research project [13].

Fig. 12 shows the percentage error calculated between the fitted surface and experimental points in Fig. 11. Individual errors never exceed ±3.3%.

3. Test and results

3.1. I-VED conductivity dependence

In this section, experiments are reported aiming to determine I-VED sensitivity with respect to alcohol concentration (or solution conductivity variation) using the Brass SELENE groove with mounted Copper electrodes shown in Fig. 3. As shown, there are three different stations of electrodes along the channel length with each station accommodating two electrode pairs, each one placed at a different height (henceforth referred to as “Up” and “Down” electrodes). The performed tests consist of filling completely first the groove with baseline aqueous solution of NaCl at different n-butanol concentrations and then recording I-VED

Table 1
Comparison between resistance measurements at 25 kHz (I-VED) and at 1 kHz (LCR bridge) for the central bottom electrode of SELENE setup. Conductivity is measured at 1 kHz with aqueous solutions of NaCl applying HANNA conductivity-meter.

Conductivity [μS/cm]	18.6	51.6	117.7	167.7
Acquisition at 25 kHz [kΩ]	30.185	10.135	4.7230	3.2375
Acquisition at 1 kHz [kΩ]	31.150	10.405	4.8950	3.4350
Deviation [%]	3.0	2.6	3.5	5.7

Table 2
Variation of I-VED resistance (kΩ) with respect to n-butanol concentration, starting with a baseline aqueous solution of NaCl of 164 μS/cm (temperature fixed at 25.5 °C).

n-BuOH % w/w	1UP[kΩ]	3UP[kΩ]	1DOWN[kΩ]	3DOWN[kΩ]
0%–1%	–	–	4.70	–
1%–2%	–	–	4.71	–
2%–3%	–	–	4.72	–
3%–4%	7.22	–	4.73	5.20
4%–5%	6.88	8.26	4.51	4.96
5%–6%	6.36	7.63	4.17	4.58
6%–7%	5.80	6.96	3.80	4.18

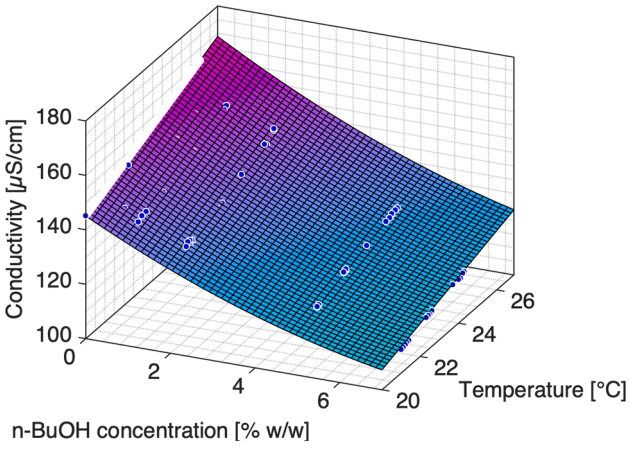

Fig. 11. 3D fitted surface of 2nd order in X and Y of the variation of conductivity with temperature and n-butanol concentration for a baseline aqueous solution of NaCl 7.7 × 10^{-3}% w/w and conductivity of 162.3 μS/cm at 25 °C.

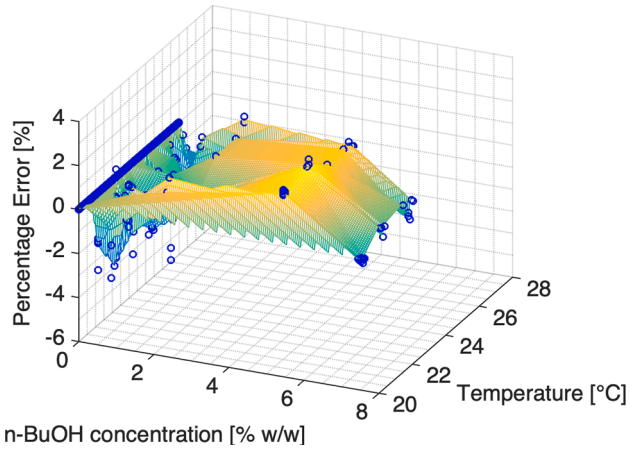

Fig. 12. 3D percentage error of the fitted surface with respect to the experimental data collected.

resistances with electrodes at position 1 Up and Down (1Up and 1Down in the figures) and electrodes at position 3 Up and Down (3Up and 3Down in the figures). With respect to the assumption made about c_f, equation (8) can be rewritten as:

$$R_{IVED} = \frac{1}{k}K \tag{9}$$

that is a hyperbolic function of conductivity k and that helps the interpolation of the experimental data shown in Fig. 13. Data are acquired with I-VED setup for different concentration solutions at isothermal conditions (25.5 °C). Data from all four pairs of electrodes are fitted with

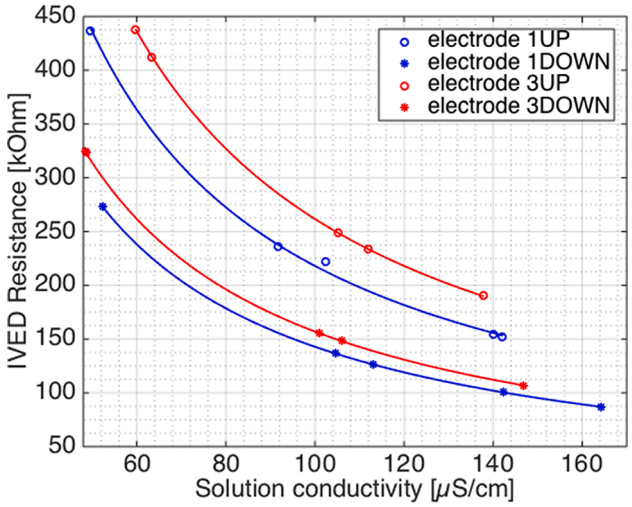

Fig. 13. Experimental data at different n-butanol concentrations (corresponding to varying solution conductivities), for different pairs of electrodes; data are obtained at 25.5 °C. Error bars representing standard deviation of measurements are smaller than the marker size.

a hyperbolic function of type y = b/x, using least squares regression, in order to find the coefficient b which corresponds to the cell factor of each electrode pair. Since the diameter of the electrode Copper wire is constant, in the definition of the cell factor the only dimension that changes with respect to UP and DOWN electrode pairs is the distance between facing electrodes.

The experimental data and fitting are plotted in Fig. 13 and the cell factors obtained from the hyperbolic fitting of the collected data are shown in Table 3. The 1UP and 3UP cell factors are quite similar as well as the 1DOWN and 3DOWN ones. This is so because there is no variation of electrodes distance at the same height and, hence, electric field is similar. On the other hand, the variation between the UP and DOWN cell factors is attributed to the different distance between the electrodes. Finally, Table 2 shows the resistance interval relative to unitary increments of n-butanol concentration, and therefore the resolution of measurements, since the x-axis of Fig. 13 is related to solution conductivity dependence on n-butanol concentration from Fig. 11. Data points in Fig. 14 represent the intersection of the 3D fitting of Fig. 11 with the plane at 25.5 °C.

In Fig. 14, it is observed that the slope of the curve decreases slightly with n-butanol concentration and as a consequence the resolution of I-VED decreases. This is also observed in Table 2 where the resistance range (and so the resolution) slightly decreases with increments of alcohol concentration.

Knowing that the sensitivity of I-VED technology is of the order of one Ohm in the linearized range of the AB, and neglecting the uncertainty due to calibration at 1 kHz (Table 1) and the surface fitting error (Fig. 12), the resulting resolution in measuring 1% of n-butanol increments varies between 0.021% and 0.026% of the I-VED scale. In the following, it is preferred to handle mixture conductivity in place of resistivity since it's more convenient when performing 2D polynomial fitting for calibration as the one shown in Fig. 11.

Based on the available data, it is possible to compare the resolution of

Table 3
(left). Cell factors for each pair of electrodes, obtained from hyperbolic fitting in Fig. 13.

	Cell Factor K [1/m]
1UP	2.1801e+04
1DOWN	1.4283e+04
3UP	2.6164e+04
3DOWN	1.5699e+04

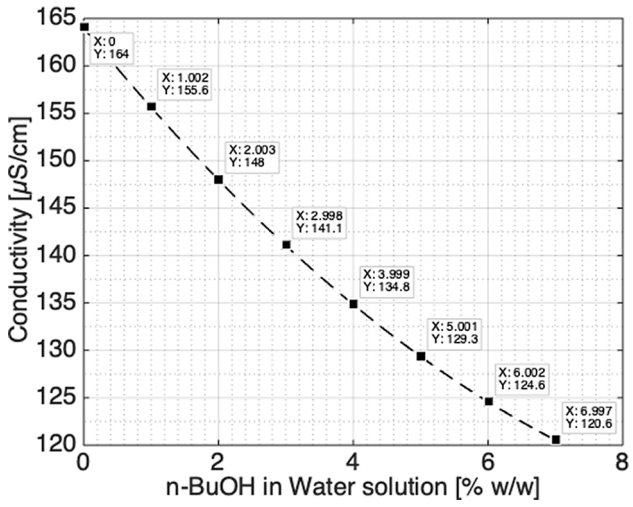

Fig. 14. Intersection of the 3D plot shown in Fig. 11 with the plane at 25.5 °C.

I-VED with the FISO and PROMETE resolutions for 1% w/w n-butanol in the solution. Data are reported in Table 4 in the form of average value with respect to the investigated range. Data are collected from 0% to 7% w/w n-butanol for I-VED (Table 2), from 0% to 3% w/w n-butanol for the Fabry-Perot sensor and from 0% to 7% w/w n-butanol for the PROMETE proposed device.

Fabry-Perot sensor has a referenced resolution of the refractive index measurement of 0.0001 RI [3], while PROMETE solution considers a linear dependence of the refractive index with alcohol concentration equal to $y = 0.0008x + 1.322$. For both technologies, the uncertainty on the refractive index is of 0.001 [2].

As can be inferred from Table 4, the resolution of I-VED for unitary increments of n-butanol is considerably better with respect to the other two technologies and may be probably comparable only with the sophisticated interferometry or spectroscopy benchtop methods. It must be stressed that I-VED technology is still under development, and further improvement is foreseen by reducing the uncertainty introduced by the calibration surface fitting in Fig. 11 and by performing calibration at excitation frequency of 25 kHz.

Apart from scale resolution, all three technologies in Table 4 present pros and cons with respect to hardware complexity, intrusiveness and type of measurement. Fiber optic techniques are very promising but intrusive and delicate whereas both Fabry-Perot and PROMETE technologies are simple to implement but provide local information over a small measuring volume that do not represent the entire cross-section of the groove. In addition, the Fabry-Perot fiber optic sensor is limited when handling high surface tension liquids that hardly flow inside the Fabry-Perot cavity resulting in a delay of the signal response with respect to liquid refractive index variations.

3.2. Liquid meniscus effect

For these tests, three different aqueous self-rewetting solutions with 1%, 3% and 6% w/w of n-butanol are used. These solutions have been prepared by mixing alcohol with a baseline aqueous solution of NaCl having conductivity of 100 μS/cm and supplied by VWR (code VWRC84139.260).

As the meniscus shape of the free surface of the liquid injected in the channel may change during tests, 4 ml of liquid are injected, which is much more than the amount needed to completely fill the groove (2.4 ml). By doing this, the electrodes are not only completely submerged to the liquid but they also lie much below the free surface of the liquid and so it is possible to neglect meniscus contribution to the measured signal at the end of the filling procedure.

The contribution of the meniscus, however, is visible in Fig. 15 during the transient period of filling the groove. In this plot, the I-VED resistance varies with time as the liquid is injected to the groove with a flow rate of 63.25 ml/h using a syringe pump. The groove is completely filled after 227 s.

The signals in Fig. 15 correspond to the DOWN electrode pair in the middle of the groove (DOWN electrode corresponding to number 8 in Fig. 4**c**). When no medium (i.e. liquid) is present between the electrodes, at the beginning of the experiment, the resistance read by I-VED is very high, but as soon as liquid is in contact with the two electrodes, the resistance drops rapidly. Once the electrodes are fully submerged and 4 ml of liquid are injected to the groove, different behaviors are observed: low alcohol concentration solutions lead to a slight increase of the resistance as the groove gets filled whereas a high alcohol concentration leads to a decrease. These trends can be explained considering that the higher is the n-butanol concentration the lower is the surface tension of the solution and this affects significantly the curvature's radius of the meniscus [19]. All in all, during the filling procedure of the groove, the meniscus influences the electrode cell factor.

3.3. Temperature effect

The following tests with I-VED technology consist of recording liquid resistance signal variation at different temperature conditions using the SELENE configuration described in Fig. 4. The same liquid mixtures and the same amount of liquids with Section 3.2 are used also herein.

Fig. 16 presents I-VED measurements for the examined mixtures at different temperatures with the groove completely filled with 4 ml of liquid. Data are averaged over 15 s of acquisition when the temperature in the groove is uniform and steady as measured by thermocouples K-type (accuracy of 0.5 °C) placed at the electrode stations. Each experiment is repeated three times and the resulting repeatability error bar is added to the respective data point. Data values are fitted with a hyperbolic function, as in Fig. 13. The plotted trends clearly show that an

Table 4
Comparison of the percentage scale resolution for different concentration measurement methods with respect to increments of 1% w/w n-butanol in the solution.

Concentration measurement method	Scale Resolution
I-VED 1DOWN electrode pair at 25.5 °C	**0.02%**
Fabry-Perot fiber optic sensor [3] at 24 °C	**10%**
PROMETE refractometry method [2] at 21.5 °C	**12.5%**

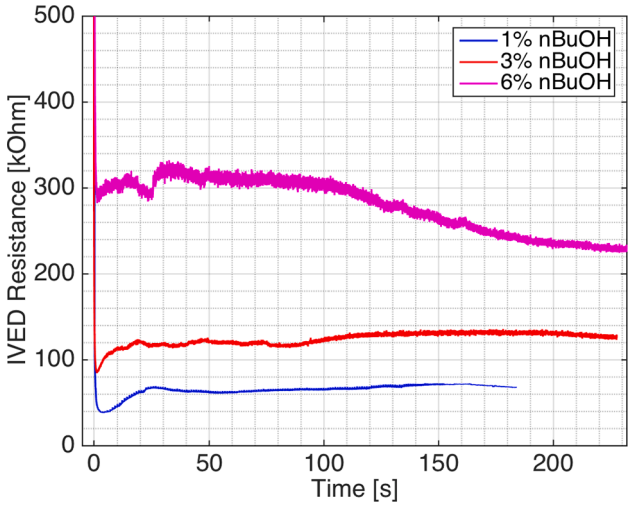

Fig. 15. Transient resistance recorded by I-VED from central-bottom electrodes during the filling of the groove with 1%, 3% and 6% w/w n-butanol using a baseline aqueous solution of NaCl of 100 μS/cm.

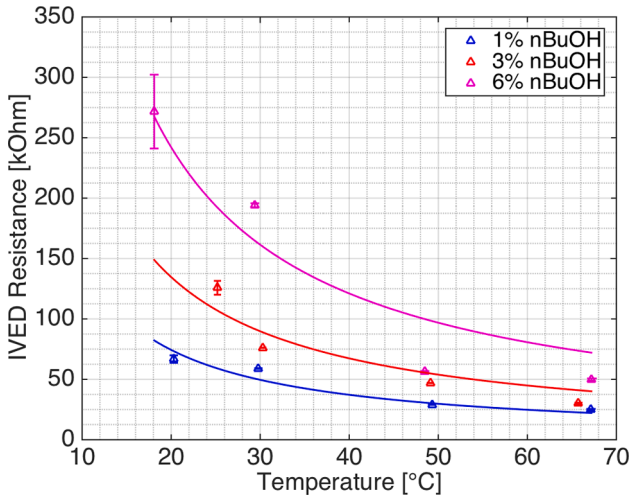

Fig. 16. Resistance recorded with I-VED central-bottom electrodes versus temperature, for isothermal conditions at various alcohol concentrations and with the groove filled completely with liquid. Repeatability error bars are displayed at data markers.

increase in temperature reduces the electrical resistance of the fluid that is normal for ohmic components. In addition, when the alcohol concentration increases, the scatter of the data increases with respect to the hyperbolic best fit curve as denoted by the error bars at the data markers. The poor repeatability at higher alcohol concentrations might be attributed in part to the lower conductivity of the solutions which reduces the measurement resolution and in part to interferences between the meniscus slope and the liquid volume between the electrode pair that become more significant. The latter is capable of affecting the cell factor of the electrode pair. This hypothesis is supported also by the trends in Fig. 15 that are irregular, too. Nevertheless, the possibility cannot be excluded that the scatter might be partially also due to Marangoni convection. When an uncontrolled thermal gradient is set along the channel (even as small as within the error of the thermal sensor), the effect of Marangoni convection may be substantial compared to the evaporation of the mixture due to the air un-tightness of the cell.

4. Conclusions

This work proposes a new diagnostic method, based on electrical impedance measurements, to retrieve concentration information for a binary mixture. The method uses I-VED hardware and processing method to provide high-resolution concentration measurements.

This concentration diagnostic has been integrated in SELENE experimental setup for testing and making observations regarding variations of the diagnostic output signal with respect to temperature and concentration variations of the mixture system. The technology is then compared with alternative methods as the refractometry methods in reflection mode created by PROMETE and the Fabry-Perot fiber optic sensor with light deflection developed by FISO.

The advantages using the proposed I-VED concentration diagnostic is associated with the possibility to completely reject the environmental electrical noise thanks to the employed high excitation frequency and to the I-VED processing algorithm itself. Apart from the calibration procedure for the I-VED method introduced in this work, the only other requirement is to increase electrical conductivity of the solution by adding low salt concentration to create a baseline solution (salt concentration ranges between 4.7×10^{-3}% and 9.5×10^{-3}% w/w). With respect to the other available techniques in the literature, I-VED shows the highest resolution in measuring an increase of alcohol concentration (n-butanol) at isothermal conditions. Experiments at different temperatures shows lower repeatability (larger data scattering) as n-butanol concentration increases, probably due to meniscus interference with the measurement itself, affecting the cell factor of the electrode pair. It will be interesting for the future to test this technology in microgravity conditions, in order to: a) assess the origin of the observed data scattering and b) obtain reliable measurements for the determination of accuracy and precision in SELENE groove configuration. If I-VED accuracy and precision is high enough, acquired signals may be further processed to provide additional information on liquid meniscus shape (in the groove section) and flow velocity (along the groove length).

CRediT authorship contribution statement

Wassilis Tzevelecos: Methodology, Validation, Formal analysis, Investigation, Writing - original draft, Visualization. **Quentin Galand:** Validation, Resources, Data curation. **Sotiris Evgenidis:** Methodology, Validation, Investigation, Writing - review & editing, Visualization. **Konstantinos Zacharias:** Methodology, Software, Validation, Investigation, Writing - review & editing. **Thodoris karapantsios:** Conceptualization, Supervision, Writing - review & editing. **Stefan Van Vaerenbergh:** Conceptualization, Supervision, Project administration, Funding acquisition, Writing - review & editing.

Declaration of Competing Interest

The authors declare that they have no known competing financial interests or personal relationships that could have appeared to influence the work reported in this paper.

Acknowledgment

This work was supported by Fonds pour la Formation à la Recherche dans l'Industrie et dans l'Agriculture (FRIA) and ESA InWIP MAP project.

References

[1] SensoTech. http://www.sensotech.com.
[2] W. Tzevelecos, Experiments in preparation of SELENE ISS microgravity research project, University of Naples Federico II, 2013. Master Thesis.
[3] E. Pinet, Fabry-Perot Fiber-Optic Sensors for Physical Parameters Measurement in Challenging Conditions, J. Sens. (2009) 1–9.
[4] T.D. Karapantsios, S.P. Evgenidis, K. Zacharias, T. Mesimeris, Method for the detection and characterization of bubbles in liquids and device therefor, resp. system, European Patent Office (2016) EP 3005942 A1.
[5] T.D. Karapantsios, S.P. Evgenidis, K. Zacharias, G. Karagiannis, Non-invasive impedance spectroscopy device for early diagnosis of Coronary Artery Disease and method therefor, European Patent Office (2017) EP 3245947 A1.
[6] S.P. Evgenidis, T.D. Karapantsios, Effect of bubble size on void fraction fluctuations in dispersed bubble flows, Int. J. Multiphas. Flow 75 (2015) 163–173.
[7] O. Oikonomidou, S.P. Evgenidis, M. Kostoglou, T.D. Karapantsios, Degassing of a pressurized liquid saturated with dissolved gas when injected to a low pressure liquid pool", Exp. Therm Fluid Sci. 96 (2018) 347–357.
[8] O. Oikonomidou, S.P. Evgenidis, C.J. Schwarz, J.W.A. van Loon, M. Kostoglou, T. D. Karapantsios, Degassing of a decompressed flowing liquid under hypergravity conditions, Int. J. Multiphas. Flow 115 (2019) 126–136.
[9] P. Gkotsis, S.P. Evgenidis, T.D. Karapantsios, Influence of Newtonian and non-Newtonian fluid behaviour on void fraction and bubble size for a gas-liquid flow of sub-millimeter bubbles at low void fractions, Exp. Therm. Fluid Sci. 109 (2019) 109912.
[10] P. Gkotsis, S.P. Evgenidis, T.D. Karapantsios, Associating void fraction signals with bubble clusters features in co-current, upward gas-liquid flow of a non-Newtonian liquid, Int. J. Multiphas. Flow 131 (2020) 103297.
[11] M. Vlachou, K. Zacharias, M. Kostoglou, T.D. Karapantsios, Droplet size distributions derived from evolution of oil fraction during phase separation of oil-in-water emulsions tracked by electrical impedance spectroscopy, Colloids Surf. A Physicochem. Eng. Asp. 586 (2020) 124292.
[12] R. Savino, A. Cecere, S. Van Vaerenbergh, Y. Abe, G. Pizzirusso, W. Tzevelecos, M. Mojahed, Q. Galand, Some experimental progresses in the study of self-rewetting fluids for the SELENE experiment to be carried in the Thermal Platform 1 hardware, Acta Astronaut. 89 (2013) 179–188.
[13] W. Tzevelecos, S. Van Vaerenbergh, Enhancing heat pipe performances using self-rewetting fluids In SELENE ground experiment. International symposium on advances in computational heat transfer, Piscataway (USA), May 2015, 2015.

[14] L.A. Bulavin, A.N. Alekseev, Yu.F. Zabashta, S.Y. Tkachev, Mechanism of Frequency- Independent Conductivity In Aqueous Solutions Of Electrolytes, Ukrainian J. Phys. 56 (6) (2011) 547–553.
[15] J. Zhang, D. Li, C. Wang, Q. Ding, An Intelligent Four-Electrode Conductivity Sensor for Aquaculture, 6th Computer and Computing Technologies in Agriculture (CCTA), Zhangjiajie (China), 2012, pp. 398-407.
[16] A. Hyldgård, D. Mortensen, K. Birkelund, O. Hansen, E.V. Thomsen, Autonomous multi-sensor micro-system for measurement of ocean water salinity, Sens. Actuator A Phys. 147 (2) (2008) 474–484.
[17] Wentworth Institute of Technology, http://myweb.wit.edu/sandinic/Research/conductivity%20v%20concentration.pdf.
[18] Y. Abe, Self-Rewetting Fluids Beneficial Aqueous Solutions, Ann. N. Y. Acad. Sci. 1077 (2006) 650–667.
[19] K.K. Cheng, C. Park, Surface tension of dilute alcohol–aqueous binary fluids: n–Butanol/water, n–Pentanol/water, and n–Hexanol/water solutions, Heat Mass Transf. 53 (7) (2017) 2255–2263.